Chapter 1
Discontinuous Galerkin model order reduction of geometrically parametrized Stokes flow

Nirav Vasant Shah, Martin Hess and Gianluigi Rozza

Abstract The present work focuses on the geometrical parametrization and the reduced order modeling of Stokes flow. We discuss the concept of a parametrized geometry and its application within a reduced order modeling technique. The full order model is based on discontinuous Galerkin method with an interior penalty formulation. We introduce broken Sobolev spaces, the jump and mean operator, as well as weak formulation require for an affine parameter dependency. The operators are transformed from a fixed domain to a parameter dependent domain using the affine parameter dependency. The proper orthogonal decomposition is used to obtain the basis of functions of the reduced order model. By using the Galerkin projection the linear system is projected onto the reduced space. During this process, offline-online decomposition is used to separate parameter dependent operation from parameter independent operations. Finally this technique is applied to an obstacle test problem. The numerical outcomes presented include the experimental error analysis and measurement of online simulation time.
Keywords Discontinuous Galerkin method, Stokes flow, Geometric parametrization, Proper orthogonal decomposition

1.1 Introduction

The subject of the mathematical applications in fluid mechanics starts with one of the variants of the Navier-Stokes equation, such as the Stokes equation. Almost all processes of fluid mechanics require considerations related to the Navier-Stokes

Nirav Vasant Shah
Scuola Internazionale Superiore di Studi Avanzati - via Bonomea, 265 - 34136 Trieste ITALY, e-mail: snirav@sissa.it

Martin Hess
Scuola Internazionale Superiore di Studi Avanzati - via Bonomea, 265 - 34136 Trieste ITALY e-mail: martin.hess@sissa.it

equations. The Navier-Stokes equation is non-linear, characterizing the flow fluctuations. However, in case of laminar flow, i.e. when fluctuations are negligible, this linearized form of the Navier-Stokes equation is the Stokes equation.

Discontinuous Galerkin method (DGM) has found traction as numerical method for the elliptic problems [6] as well as the hyperbolic problems [2]. This is due to its several advantages over the Finite Element Method (FEM) and the Finite Volume Method (FVM). In fact, DGM is considered as the combination of FEM and FVM. DGM uses polynomial approximation of a suitable degree providing higher accuracy as well as allows discontinuity at the interface, by the concept of numerical flux, allowing greater flexibility. This fact makes DGM naturally attractive to problems, such as shock capturing, due to presence of steep gradients or discontinuities. Additionally, since the Dirichlet conditions are applied as boundary penalty, it avoids necessity to construct a subspace of Sobolev space such as in case of FEM. Several variants of DGM exist based on computational advantages such as sparsity pattern or extension of computational stencil, need for stabilization, complexity of numerical implementation etc.

Geometric parametrization has emerged as a important application of the Parametric Partial Differential Equations (PPDEs) and as alternative to the shape optimization. The concept of geometric parametrization allows to transfer operator evaluated on one geometric domain to another geometric domain efficiently. For linear equations, this means exploiting affine parameter dependence as will be shown in later section. Model Order Reduction (MOR) on the other hand allows reducing the size of the system to be solved by working with the smaller system containing only dominant components and by discarding the non-dominant components. It is pertinent to mention that identifying the "dominant" components is critical to the success of the model order reduction strategy. Optimization of engineering components using geometric parametrization combined with MOR for PPDEs has given quite useful results in the fields such as mechanical, naval and aeronautic designs. Also, the faster computations obtained by MOR has helped in many query context, real time computation and quick transfer of computational results to industrial problems.

As evident from above advantages, the application of geometric parametrization and reduced order modeling to discontinuous Galerkin method will remain at the forefront of scientific work. The present work is aimed to contribute to this emerging field. We first introduce the notion of geometric parametrization. We subsequently introduce Discontinuous Galerkin Interior Penalty Method (DG-IPM) for the stokes flow. We then explain exploiting the affine parameter dependence and its application in the context of the offline-online decomposition. Proper Orthogonal Decomposition (POD) is applied to construct the reduced basis space and Galerkin projection is applied to project the system of equations on the reduced basis space. Finally we present an obstacle test problem, to which the introduced method is applied. The numerical outcomes provide overview of the potential of the presented method.

1.2 Geometric parametrization

Consider domain $\Omega = \Omega(\mu) \in \mathbb{R}^d$ as open bounded domain. The parameter set $\mu \in \mathbb{P}$, where $\mathbb{P}$ is parameter space, completely characterizes the domain. Also, consider a parameter set $\bar{\mu} \in \mathbb{P}$, as the known parameter set and $\Omega(\bar{\mu})$ as the reference domain, whose configuration is completely known. The invertible mapping $\boldsymbol{F}(\cdot, \mu) : \Omega(\bar{\mu}) \rightarrow \Omega(\mu)$ links reference domain and parametrized domain. In the case of affine transformation, $\boldsymbol{F}$ is of the form,

$$x = \boldsymbol{F}(\hat{x}, \mu) = \boldsymbol{G}_F(\mu)\hat{x} + c_F(\mu) \; ; \forall x \in \Omega \, , \; \hat{x} \in \Omega(\bar{\mu}) \, . \tag{1.1}$$

The boundary of $\Omega(\mu)$, that is $\partial\Omega(\mu)$ is divided into Neumann boundary $\Gamma_N(\mu)$ and Dirichlet boundary $\Gamma_D(\mu)$ i.e. $\partial\Omega(\mu) = \Gamma_N(\mu) \cup \Gamma_D(\mu)$. The domain $\Omega(\mu)$ is divided into n_{su} subdomains such that $\Omega(\mu) = \bigcup_{i=1}^{n_{su}} \Omega_i(\mu)$, $\Omega_i(\mu) \bigcap \Omega_j(\mu) = \emptyset$, for $i \neq j$.

1.3 Discontinuous Galerkin formulation

Each subdomain is divided into N_{el} number of triangular elements τ_k such that $\Omega = \bigcup_{k=1}^{N_{el}} \tau_k$. The triangulation $\mathcal{T}$ is the set of all triangular elements i.e. $\mathcal{T} = \{\tau_k\}_{k=1}^{N_{el}}$. The internal boundary $\Gamma = \bigcup_{k=1}^{N_{el}} \partial\tau_k \backslash \partial\Omega$. The vertices of triangles $\tau_k{}_{k=1}^{N_{el}}$ are called nodes. $\overrightarrow{n}$ is the outward pointing normal to an edge of element.

The Stokes's equation in strong form can be stated as,

$$-\nu\Delta\overrightarrow{u} + \nabla p = \overrightarrow{f} \, , \text{ in } \Omega \, , \tag{1.2}$$

$$\nabla \cdot \overrightarrow{u} = 0 \, , \text{ in } \Omega \, , \tag{1.3}$$

$$\overrightarrow{u} = \overrightarrow{u}_D \, , \text{ on } \Gamma_D \, , \tag{1.4}$$

$$-p\overrightarrow{n} + \nu\overrightarrow{n} \cdot \nabla\overrightarrow{u} = \overrightarrow{t} \, , \text{ on } \Gamma_N \, . \tag{1.5}$$

The velocity vector field $\overrightarrow{u}$ and pressure scalar field p are the unknowns. ν is the material property known as kinematic viscosity. Vector $\overrightarrow{f}$ is external force term or source term. $\overrightarrow{u}_D$ is the Dirichlet velocity and $\overrightarrow{t}$ is the Neumann value.

Before introducing weak form let us introduce broken Sobolev spaces for variables.

The space for velocity is

$$\mathbb{V} = \{\overrightarrow{\phi} \in (L^2(\Omega))^d | \; \overrightarrow{\phi} \in (P^D(\tau_k))^d \, , \; \tau_k \in \mathcal{T}\} \, . \tag{1.6}$$

The space for pressure is

$$\mathbb{Q} = \{\psi \in (L^2(\Omega))|\ \psi \in (P^{D-1}(\tau_k))\ ,\ \tau_k \in \mathcal{T}\}\ . \tag{1.7}$$

Here, $P^D(\tau_k)$ denotes space of polynomials of degree at most $D \geq 2$ over τ_k.

In finite dimensional or discrete system, velocity approximation $\overrightarrow{u}_h(x)$ and pressure approximation $p_h(x)$ at any point $x \in \Omega$ are given by,

$$\overrightarrow{u}_h(x) = \sum_{i=1}^{u_{ndofs}} \overrightarrow{\phi}_i \hat{u}_i\ ,\ p_h(x) = \sum_{i=1}^{p_{ndofs}} \psi_i \hat{p}_i\ , \tag{1.8}$$

where $\hat{u}_i$'s and $\hat{p}_i$'s are coefficients of velocity basis functions and pressure basis functions respectively.

We expect that $\overrightarrow{u}_h \rightarrow \overrightarrow{u}$ and $p_h \rightarrow p$ as $u_{ndofs} \rightarrow \infty$ and $p_{ndofs} \rightarrow \infty$ respectively. Considering scope of present work, the convergence analysis will not be discussed here. The readers are advised to refer to [1], [7].

In the subsequent sections $(\cdot)$, $(\cdot)_{\Gamma_D}$, $(\cdot)_{\Gamma_N}$, $(\cdot)_{\Gamma}$ represent the L^2 scalar product over $\Omega, \Gamma_D, \Gamma_N, \Gamma$ respectively. The jump operator $[\cdot]$ and the average operator $\{\cdot\}$ are important concepts in DGM formulation and are required to approximate the numerical flux. Different definitions are used in literatures for jump and mean operators. We use the jump and average operators as defined by [5].

The weak form of Stokes equation is as follow,

$$a_{IP}(\overrightarrow{u}, \overrightarrow{\phi}) + b(\overrightarrow{\phi}, p) + \left(\{p\}, [\overrightarrow{n} \cdot \overrightarrow{\phi}]\right)_{\Gamma \cup \Gamma_D} = l_{IP}(\overrightarrow{\phi})\ , \tag{1.9}$$

$$\begin{aligned} a_{IP}(\overrightarrow{u}, \overrightarrow{\phi}) = &\left(\nabla\overrightarrow{u}, \nabla\overrightarrow{\phi}\right) + C_{11}\left([\overrightarrow{u}], [\overrightarrow{\phi}]\right)_{\Gamma \cup \Gamma_D} \\ &-\nu\left(\{\nabla\overrightarrow{u}\}, [\overrightarrow{n} \otimes \overrightarrow{\phi}]\right)_{\Gamma \cup \Gamma_D} - \nu\left([\overrightarrow{n} \otimes \overrightarrow{u}], \{\nabla\overrightarrow{\phi}\}\right)_{\Gamma \cup \Gamma_D}\ , \end{aligned} \tag{1.10}$$

$$b(\overrightarrow{\phi}, \psi) = -\int_{\Omega} \psi \nabla \cdot \overrightarrow{\phi}\ , \tag{1.11}$$

$$l_{IP}(\overrightarrow{\phi}) = \left(\overrightarrow{f}, \overrightarrow{\phi}\right) + \left(\overrightarrow{t}, \overrightarrow{\phi}\right)_{\Gamma_N} + C_{11}\left(\overrightarrow{u}_D, \overrightarrow{\phi}\right)_{\Gamma_D} - \left(\overrightarrow{n} \otimes \overrightarrow{u}_D, \nu\nabla\overrightarrow{\phi}\right)_{\Gamma_D}\ . \tag{1.12}$$

The penalty parameter $C_{11} > 0$ in $a_{IP}(\overrightarrow{u}, \overrightarrow{\phi})$ is an empirical constant to be kept large enough to maintain coercivity of bilinear form.

The weak for of continuity equation is as follow,

$$b(\overrightarrow{u}, \psi) + (\psi, [\overrightarrow{n} \cdot \overrightarrow{u}])_{\Gamma \cup \Gamma_D} = (\psi, \overrightarrow{n} \cdot \overrightarrow{u}_D)_{\Gamma_D}\ . \tag{1.13}$$

In discrete form system of equations can be written as,

$$\underbrace{\begin{pmatrix} \boldsymbol{A} & \boldsymbol{B} \\ \boldsymbol{B}^T & 0 \end{pmatrix}}_{\text{Stiffness matrix}} \underbrace{\begin{pmatrix} U \\ P \end{pmatrix}}_{\text{Solution vector}} = \underbrace{\begin{pmatrix} F_1 \\ F_2 \end{pmatrix}}_{\text{Right hand side (Known)}} . \tag{1.14}$$

Here, $\boldsymbol{A}_{ij} = a_{IP}(\overrightarrow{\phi}_i, \overrightarrow{\phi}_j)$, $\boldsymbol{B}_{ij} = b(\overrightarrow{\phi}_i, \psi_j) + \left(\{\psi_j\}, [n \cdot \overrightarrow{\phi}_i]\right)_{\Gamma \cup \Gamma_D}$, $F_1 = l_{IP}(\overrightarrow{\phi}_i)$ and $F_2 = \left(\psi_j, \overrightarrow{n} \cdot \overrightarrow{u}_D\right)_{\Gamma_D}$. The column vectors U and P are coefficients $\hat{u}$'s and $\hat{p}$'s from equation (1.8).

1.4 Affine expansion

We evaluate and solve the Stokes equation weak formulation on reference domain $\Omega(\bar{\mu})$. Given a parameter $\mu \neq \bar{\mu}$ we need to evaluate the linear systems of equation (1.14) on new domain $\Omega(\mu)$. To accomplish this we use affine expansion using linear nature of equation and diving $\Omega(\bar{\mu})$ into triangular subdomains $\Omega_i(\bar{\mu})$, $i = \{1, 2, \ldots, n_{su}\}$ as explained earlier in the section geometric parametrization [Section 1.2]. The affine expansion of operators is essentially change of variable and has been explained in literatures such as [4]. However it is pertinent to explain two expansions as specific to DGM formulation.

- In order to transfer the terms containing jump and average operator following approach is used in present analysis.

$$\left(\{\nabla\overrightarrow{\phi}\}, \left[\overrightarrow{n} \otimes \overrightarrow{\phi}\right]\right) = \left(\nabla\overrightarrow{\phi}^+, \overrightarrow{n}^+ \otimes \overrightarrow{\phi}^+\right) + \left(\nabla\overrightarrow{\phi}^+, \overrightarrow{n}^- \otimes \overrightarrow{\phi}^-\right) + \left(\nabla\overrightarrow{\phi}^-, \overrightarrow{n}^+ \otimes \overrightarrow{\phi}^+\right) + \left(\nabla\overrightarrow{\phi}^-, \overrightarrow{n}^- \otimes \overrightarrow{\phi}^-\right) .$$

  Each term on right hand side of above equation can now be transformed using affine map.

- The coercivity term $C_{11}\left([\overrightarrow{\phi}], [\overrightarrow{u}]\right)_{\Gamma \cup \Gamma_D}$ is not transformed but used as evaluated on reference domain $\Omega(\bar{\mu})$. The affine transformation is given by,

$$C_{11}\left([\overrightarrow{\phi}(\hat{x}), \overrightarrow{u}(\hat{x})]\right)_{\Gamma(\mu) \cup \Gamma_D(\mu)} = C_{11}\alpha\left([\overrightarrow{\phi}(\boldsymbol{F}(\hat{x})), \overrightarrow{u}(\boldsymbol{F}(\hat{x}))]\right)_{\Gamma(\bar{\mu}) \cup \Gamma_D(\bar{\mu})} ,$$
$$\alpha = \frac{\text{length of } (\Gamma(\mu) \cup \Gamma_D(\mu))}{\text{length of } (\Gamma(\bar{\mu}) \cup \Gamma_D(\bar{\mu}))} , \ \hat{x} \in \Omega(\bar{\mu}) , \ x \in \Omega(\mu) .$$

  Since, C_{11} is empirical coefficient replacing $C_{11}\alpha$ with C_{11} will not change the formulation as long as coercivity of a_{IP} over parameter space $\mathbb{P}$ is maintained.

1.5 Reduced basis method

In this section snapshot proper orthogonal decomposition method and offline-online decomposition are briefly described. For detailed explanation we refer to [4].

1.5.1 Snapshot proper orthogonal decomposition

Firstly, the solutions based on $\mu_n, n \in \{1, ..., n_s\}$ are calculated i.e. n_s snapshots are generated. The velocity snapshots and the pressure snapshots are stored in $\boldsymbol{S}_v \in \mathbb{R}^{u_{ndofs} \times n_s}$, $\boldsymbol{S}_p \in \mathbb{R}^{p_{ndofs} \times n_s}$ respectively. Let us also introduce inner product matrices $\boldsymbol{M}_v \in \mathbb{R}^{u_{ndofs} \times u_{ndofs}}$ and $\boldsymbol{M}_p \in \mathbb{R}^{p_{ndofs} \times p_{ndofs}}$.

$$\boldsymbol{M}_{v,ij} = \int_\Omega \overrightarrow{\phi}_i \cdot \overrightarrow{\phi}_j + \sum_{k=1}^{N_{el}} \int_{\tau_k} \nabla \overrightarrow{\phi}_i : \nabla \overrightarrow{\phi}_j \ , \ i, j = 1, \ldots, u_{ndofs} \ ,$$

$$\boldsymbol{M}_{p,ij} = \int_\Omega \psi_i \psi_j \ , \ i, j = 1, \ldots, p_{ndofs} \ .$$

The dimension of reduced basis is denoted as N and it is asserted that $N << u_{ndofs}, N < n_s$. Next, the spectral decomposition of snapshots is performed.

$$\boldsymbol{S}_v^T \boldsymbol{M}_v \boldsymbol{S}_v = \boldsymbol{V} \boldsymbol{\Theta} \boldsymbol{V}^T \ . \tag{1.15}$$

The columns of $\boldsymbol{V}$ are eigenvectors and Θ has eigenvalues θ_i , $1 \leq i, j \leq n_s$ in sorted order such that, $\Theta_{ij} = \theta_i \delta_{ij}$.

The reduced basis is formed by the linear combination of the snapshot vector,

$$\boldsymbol{B}_v = \boldsymbol{S}_v \boldsymbol{A} \ , \ \boldsymbol{A} \in \mathbb{R}^{n_s \times N} \ . \tag{1.16}$$

the reduced basis for velocity basis function $\overrightarrow{\phi}_N$ is formed by,

$$\overrightarrow{\phi}_N = \overrightarrow{\phi}^T \boldsymbol{B}_v \ . \tag{1.17}$$

Considering orthonormality of reduced basis with respect to inner product given by $\boldsymbol{M}_v$,

$$\boldsymbol{B}_v = \boldsymbol{S}_v \boldsymbol{V} \boldsymbol{\Theta}^{-\frac{1}{2}} \boldsymbol{R} \ , \ \boldsymbol{R} = [\boldsymbol{I}; \boldsymbol{0}_{(n_s - N) \times N}] \ , \tag{1.18}$$

where, $\boldsymbol{I}_{N \times N}$ is identity matrix of size $N \times N$. The reduced basis space $\boldsymbol{B}_p$ can be generated in similar manner using pressure snapshots $\boldsymbol{S}_p$ and inner product matrix $\boldsymbol{M}_p$.

1.5.2 Galerkin reduced basis formulation

The discrete system of equations is projected onto reduced space as,

$$\underbrace{\begin{pmatrix} \boldsymbol{B}_v^T \boldsymbol{A}(\mu)\boldsymbol{B}_v & \boldsymbol{B}_v^T \boldsymbol{B}(\mu)\boldsymbol{B}_p \\ \boldsymbol{B}_p^T \boldsymbol{B}(\mu)^T \boldsymbol{B}_v & \boldsymbol{0} \end{pmatrix}}_{\tilde{K}} \underbrace{\begin{pmatrix} U_N \\ P_N \end{pmatrix}}_{\zeta} = \underbrace{\begin{pmatrix} \boldsymbol{B}_v^T F_1(\mu) \\ \boldsymbol{B}_p^T F_2(\mu) \end{pmatrix}}_{\tilde{F}}, \tag{1.19}$$

and accordingly following the variational form for the reduced degrees of freedom ζ is solved,

$$\tilde{\boldsymbol{K}}\zeta = \tilde{F} \ . \tag{1.20}$$

The parameter dependent matrices in equation (1.19) are evaluated by using affine decomposition. The solution vectors U and P (equation (1.14)) are then computed as,

$$U = \boldsymbol{B}_v U_N \ , \ P = \boldsymbol{B}_p P_N \ . \tag{1.21}$$

1.5.3 Offline-online procedure

During the offline phase n_s snapshots are computed and reduced basis spaces $\boldsymbol{B}_v$ and $\boldsymbol{B}_p$ are created as outlined in section 1.5.1. During the online phase the systems of equations are projected on reduced space using Galerkin projection. During the online phase, the smaller systems of equation obtained by Galerkin projection is solved and the reduced basis solution is computed as outlined in section 1.5.2.

1.6 Numerical example

We perform the POD-Galerkin method as mentioned in section 1.5.1 - section 1.5.2. The numerical experiments were performed using RBmatlab [3]. The reference domain $\Omega(\bar{\mu})$ is the unit square domain $[0,1] \times [0,1]$ with triangle with vertices $(0.3, 0), (0.5, 0.3), (0.7, 0)$ as obstacle. The geometric parameters are coordinates of tip of the obstacle i.e. $\bar{\mu} = (0.5, 0.3)$. The boundary $x = 0$ is Dirichlet boundary with inflow velocity at point $(0, y)$ as $u = (y(1-y), 0)$. The boundary $x = 1$ is a Neumann boundary with zero Neumann value i.e. $\overrightarrow{t} = (0, 0)$. Other boundaries are Dirichlet boundary with no slip condition. The source term is $\overrightarrow{f} = (0, 0)$.

The training set was generated by random generation of 100 parameters between the interval $[0.4, 0.6] \times [0.4, 0.6]$. The test set contained 10 random parameters between the interval $[0.4, 0.6] \times [0.4, 0.6]$. For velocity basis function polynomial of degree $P^D = 2$ and for pressure basis function polynomial of degree $P^{D-1} = 1$ was used. The number of velocity degrees of freedom and pressure degrees of freedom were $u_{ndofs} = 4704$ and $p_{ndofs} = 1176$ respectively.

Figure 1.1 shows solution computed by DGM and POD at parameter value $(0.47, 33)$. Figure 1.2 shows error vs size of reduced basis space. As can be seen the error drops with increasing size of basis function, however, this has to be at affordable cost of increased online simulation time. The online simulation time for reduced basis with 10 basis functions was 2.25 seconds, which is 19.5 times faster than DGM model.

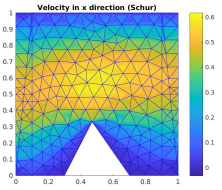

(a) Velocity $x-$direction DG solution

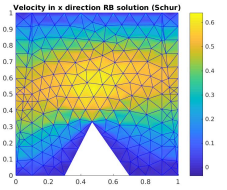

(b) Velocity $x-$direction RB solution

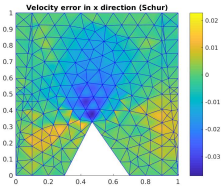

(c) $x-$component of Velocity absolute error $\overrightarrow{u}_h - \overrightarrow{u}_N$

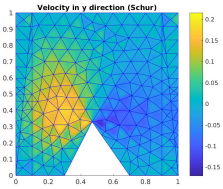

(d) Velocity $y-$direction DG solution

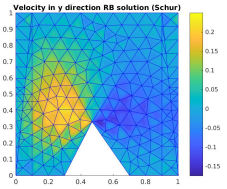

(e) Velocity $y-$direction RB solution

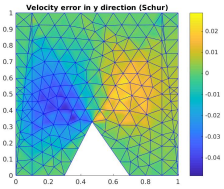

(f) $y-$component of Velocity absolute error $\overrightarrow{u}_h - \overrightarrow{u}_N$

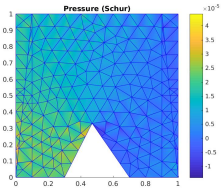

(g) Pressure DG solution

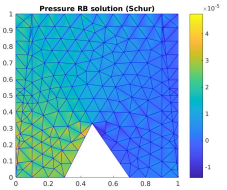

(h) Pressure RB solution

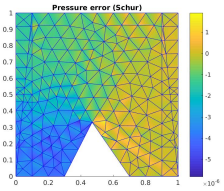

(i) Pressure absolute error $p_h - p_N$

Fig. 1.1: DG and RB solution $[\mu_x \ \mu_y] = [0.47 \ 0.33]$

References

[1] Antonietti, Paola F, Pacciarini, Paolo, Quarteroni, Alfio (2016) A discontinuous galerkin reduced basis element method for elliptic problems. ESAIM: M2AN 50(2):337–360, DOI 10.1051/m2an/2015045, URL `https://doi.org/10.1051/m2an/2015045`

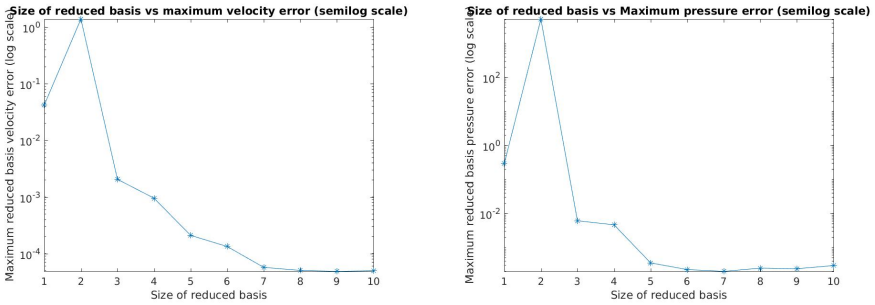

(a) Size of reduced basis space vs. Maximum relative error in velocity with inner product induced by $\boldsymbol{M}_v$

(b) Size of reduced basis space vs. Maximum relative error in pressure with inner product induced by $\boldsymbol{M}_p$

Fig. 1.2: Size of reduced basis vs Maximum relative error

[2] Dolejší V, Feistauer M (2015) Discontinuous Galerkin Method: Analysis and Applications to Compressible Flow. Springer Series in Computational Mathematics, Springer International Publishing, URL https://books.google.es/books?id=Pj4wCgAAQBAJ

[3] Drohmann M, Haasdonk B, Kaulmann S, Ohlberger M (2012) A software framework for reduced basis methods using dune-rb and rbmatlab. In: Dedner A, Flemisch B, Klöfkorn R (eds) Advances in DUNE, Springer Berlin Heidelberg, Berlin, Heidelberg, pp 77–88

[4] Hesthaven JS, Rozza G, Stamm B (2015) Certified Reduced Basis Methods for Parametrized Partial Differential Equations, 1st edn. Springer Briefs in Mathematics, Springer, Switzerland, DOI 10.1007/978-3-319-22470-1

[5] Kanschat G, Schoetzau D (2008) Energy norm a posteriori error estimation for divergenceâĂŘfree discontinuous galerkin approximations of the navierâĂŞstokes equations. International Journal for Numerical Methods in Fluids 57:1093 – 1113, DOI 10.1002/fld.1795

[6] Peraire J, Persson PO (2008) The compact discontinuous galerkin (cdg) method for elliptic problems. SIAM Journal on Scientific Computing 30(4):1806–1824, DOI 10.1137/070685518, URL https://doi.org/10.1137/070685518

[7] Riviere B (2008) Discontinuous Galerkin Methods for Solving Elliptic and Parabolic Equations: Theory and Implementation. Frontiers in Applied Mathematics, Cambridge University Press, URL https://books.google.de/books?id=GY4GtnDCaSQC